



Investigation of luminescence and scintillation properties of a ZnS–Ag/⁶LiF scintillator in the 7–295 K temperature range

V.B. Mikhailik^{a,b,*}, S. Henry^a, M. Horn^a, H. Kraus^a, A. Lynch^a, M. Pipe^a

^a Department of Physics, University of Oxford, Keble Road, Oxford OX1 3RH, UK

^b Diamond Light Source, Harwell Science Campus, Didcot OX11 0DE, UK

ARTICLE INFO

Article history:

Received 22 June 2012

Received in revised form

28 August 2012

Accepted 5 September 2012

Keywords:

ZnS–Ag

Cryogenic scintillator

Neutron detection

Recombination decay kinetics

ABSTRACT

The luminescence and scintillation properties of ZnS–Ag/⁶LiF were studied in the 7–295 K temperature range to evaluate the suitability of the scintillator for neutron detection at very low temperature (< 1 K). It is shown that decrease of temperature has little effect upon principal luminescence and scintillation characteristics of ZnS–Ag: the changes of emission intensity are small for photoexcitation and negligible for excitation with α -particles. The recombination kinetics of the scintillation decay exhibits modest shortening of the fast decay time constant, from 4.52 to 3.35 μ s with cooling to 10 K. It is concluded that ZnS–Ag/⁶LiF is a promising scintillator for cryogenic application.

© 2012 Elsevier B.V. All rights reserved.

1. Introduction

Zinc sulfide (ZnS) activated with Ag⁺ ions is known for its brilliant blue luminescence under excitation with high energy photons, electrons or ions. Discovered more than a century ago [1] it remains one of the most efficient among the practical phosphors and scintillators: about 20% of absorbed energy is converted into visible emission [2], resulting in a light yield of 75,000 photons/MeV [3]. It has thus been associated with important scientific discoveries and technical innovations such as Rutherford's studies of radioactivity [4] and the development of cathode ray tubes [5]. Despite significant progress with ionizing radiation detectors, ZnS–Ag remains the longest-in-use and yet unchallenged scintillation material employed for detection of α -particles and neutrons.

Due to the importance of ZnS–Ag for practical applications, there is a long history of research on the luminescence and scintillation properties of this material, with key results summarized in review papers and books (see e.g. [5–10]). The mechanism behind the intense emission band at 450 nm is now well established as being due to recombination of spatially separated donor–acceptor pairs. A characteristic feature of such recombination luminescence is a long decay time, spanning the range from milliseconds to a few seconds [11,12].

It is the high scintillation yield for α -particles that makes the combination of ZnS–Ag with ⁶LiF very efficient for the detection of neutrons. Alpha particles created in ⁶LiF through a ⁶Li(n, α)t reaction cause scintillations of ZnS–Ag which is easy to detect [3,13]. Currently this material is widely used for neutron detection in different applications including imaging [14,15]. Therefore the luminescence and scintillation properties of ZnS–Ag/⁶LiF at ambient conditions have been extensively studied and characterized [16–19]. However, no results on the low temperature properties of this material have been published so far, mainly due to lack of motivation for low temperature applications.

An application for neutron detectors at temperatures < 1 K emerged recently from fundamental physics experiments, such as the direct dark matter search EURECA [20] and the search for a non-zero electric dipole moment of the neutron CryoEDM [21]. Both experiments use cryogenic techniques to achieve enhanced sensitivity: CryoEDM needs a cryogenic neutron detector to accurately count the number of ultra-cold neutrons, and EURECA could benefit from precise neutron background monitoring close to the cryogenic dark matter detectors.

It has been shown that many scintillation materials are suitable for operation at cryogenic temperatures: the scintillation light yield usually increases with cooling, however a substantial increase of the long scintillation time constant is an issue [22]. The detection of scintillations using a commercial photomultiplier tube at low temperatures has also been demonstrated [23]. It is therefore an obvious next step to design a neutron detector, based on scintillation detection and capable of operating at cryogenic temperatures. For this to work, a scintillator needs to be identified

* Corresponding author at: Department of Physics, University of Oxford, Keble Road, Oxford OX1 3RH, UK. Tel.: +44 01235 778801.

E-mail addresses: v.mikhailik@physics.ox.ac.uk, vmikhail@hotmail.com (V.B. Mikhailik).

for which the increase of scintillation time constant at low temperature is not too great. This motivated the present studies of the luminescence and scintillation properties of ZnS–Ag/⁶LiF over a wide temperature range.

2. Experiment

In this study we characterize ZnS–Ag/⁶LiF produced by Applied Scintillation Technologies (Harlow, UK). To measure the scintillation properties as functions of temperature, the 5 × 5 mm² scintillator sample with thickness of about 1 mm was placed in a helium flow cryostat and excited by α -particles from an ²⁴¹Am source (activity 33 kBq). The event rate was adjusted by placing a stainless steel aperture with a 0.1 mm diameter hole between the sample and source. Details of the experimental setup, data analysis procedure and features of the multiphoton counting technique used in this study are described elsewhere [24].

The measurements of the luminescence properties were carried out using vacuum ultraviolet (VUV) synchrotron radiation at the SUPERLUMI station at HASYLAB [25]. The sample was glued to the sample holder of a helium flow cryostat. For the measurements of excitation spectra, the emission band was selected by a SpectraPro308 (Action Research) monochromator and monitored using a Hamamatsu R6358P photomultiplier tube. The excitation spectra were normalized to equal intensity of the synchrotron radiation by dividing by the response of a sample of sodium salicylate that has constant quantum yield over the energy range of interest. The emission spectra were measured at fixed excitation energy using a liquid nitrogen cooled CCD camera (Princeton Instruments). The spectra presented here are corrected for the spectral response of the detection system.

3. Results and discussion

3.1. Luminescence properties

Fig. 1 shows the luminescence spectra of ZnS–Ag/⁶LiF measured at different temperatures under excitation with 4.1 eV photons. According to current understanding of the luminescence mechanism of ZnS–Ag excitation, high-energy photons promote electrons to the conduction band and thus create holes in the valence band. The holes are then trapped by Ag⁺ which replaces regular Zn²⁺ ions on their sites, while electrons can be captured

by shallow levels of charge-compensating sites associated with either impurities or intrinsic defects. Subsequent recombination of electrons with these holes results in the characteristic blue emission of ZnS–Ag phosphor [6–12]. The decrease of temperature results in an increase of the emission intensity that is a typical feature of recombination luminescence. The temperature evolution of luminescence is controlled by thermal quenching as the probability of non-radiative recombination increases with temperature. Due to the relatively high activation energy of thermal quenching in ZnS–Ag the luminescence at room temperature remains at a relatively high intensity (see inset in Fig. 1); and that facilitates the wide-ranging application of this materials.

The excitation spectra of ZnS–Ag/⁶LiF at room temperature and 7 K are displayed in Fig. 2. Our results are in good agreement with earlier measurements of a ZnS–Ag phosphor [26]. The main features of the excitation spectra can be explained on the basis of present knowledge of the band structure of ZnS [27,28], using a phenomenological model of the energy conversion process in solids [29,30]. The sharp rise in the excitation spectra corresponds to the band gap energy of zinc sulfide, E_g , which is assigned to 3.8 eV [31]. When the excitation photon energy increases, the kinetic energy, and hence mean distance between the electrons and holes also increases. As the electrons taking part in the recombination must migrate to the luminescence center they can be lost by decaying through non-radiative surface recombination [32]. This effect reduces the probability of luminescence recombination and explains the decrease of the light output over the 4–11 eV energy range. Because the ZnS–Ag/⁶LiF sample used in this study contains an organic binder it is reasonable to expect that some VUV photons may be absorbed by this binder thus reducing the light yield further.

The structure observed in the excitation spectra at higher energies can be related to the features of the valence band of ZnS. Measurements of the X-ray photoelectron emission spectra show that the valence band of ZnS consists of three bands with maxima at around 2.6, 4.9 and 12.4 eV (energies are quoted with respect to the top of the valence band) [28]. They originate from the outermost cation and anion s- and p-electrons. By adding the band gap energy to these values one finds that the bands in the excitation spectra of ZnS–Ag marked A, B and C correspond to the position of the valence band–conduction band transitions at 6.4, 8.7 and 16.2 eV (see Fig. 2).

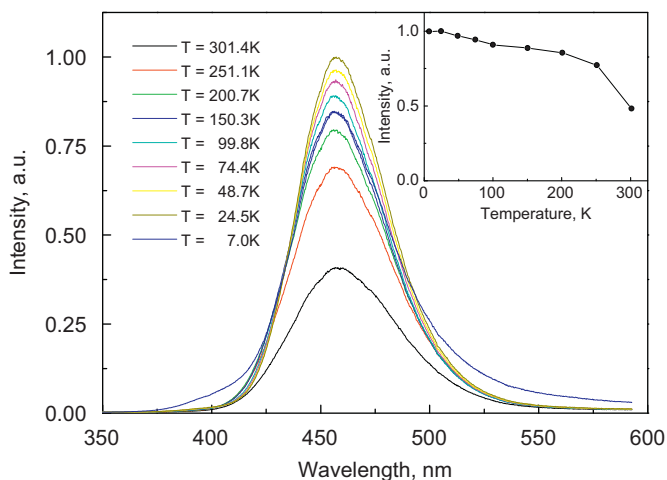


Fig. 1. Luminescence spectra of ZnS–Ag/⁶LiF measured at different temperatures under excitation with 4.1 eV photons. The inset shows the total luminescence intensity as function of temperature.

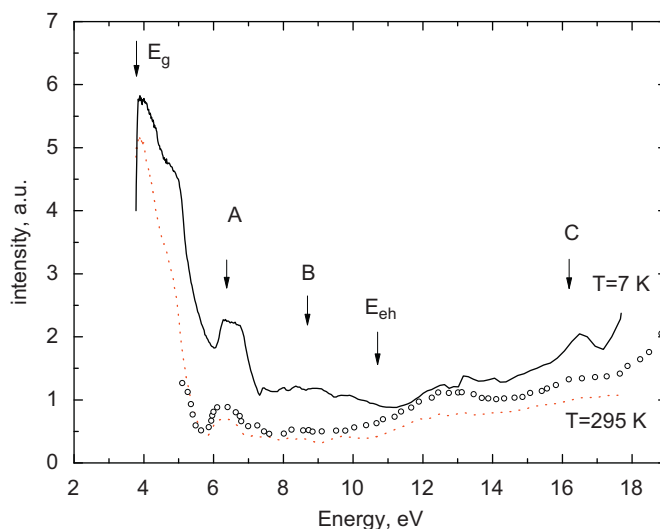


Fig. 2. Excitation spectra of ZnS–Ag/⁶LiF monitored at 450 nm for temperatures of 295 K and 7 K. Open circles show the excitation spectrum of ZnS–Ag at room temperature from [26].

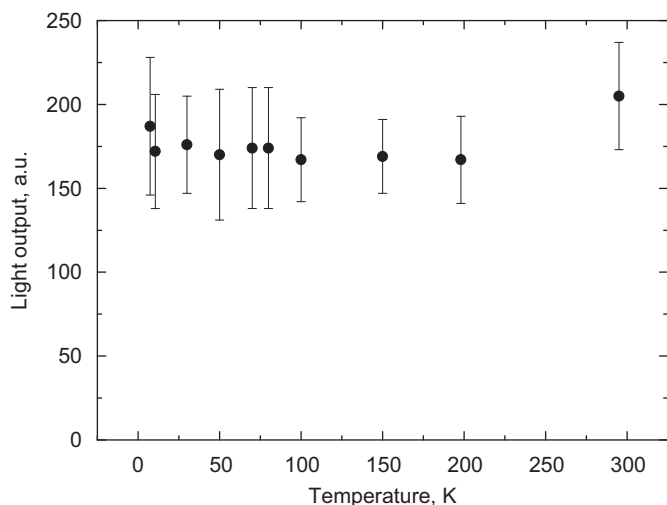


Fig. 3. Temperature dependence of scintillation light output of ZnS-Ag/⁶LiF measured at excitation with 5.5 MeV α -particles (²⁴¹Am).

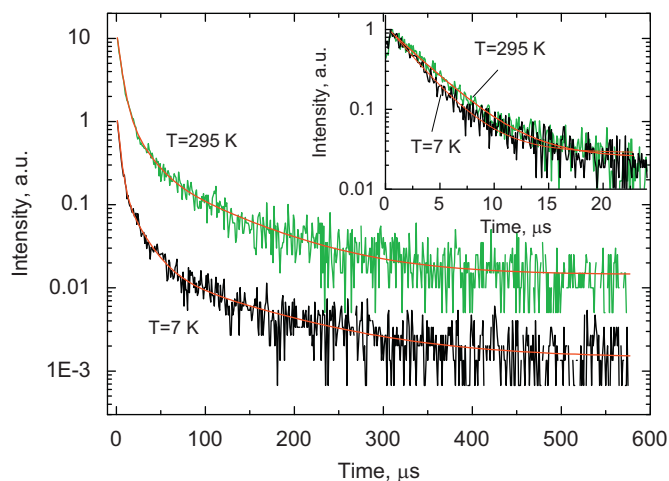


Fig. 4. Normalized scintillation decay curves of ZnS-Ag/⁶LiF measured at $T=295$ and 7 K (the graphs are vertically shifted for clarity). Lines show the fit to experimental data using the sum of three exponential functions (see text). Parameters of the fit are listed in Table 1. The inset shows the initial part of the decay curves.

The mentioned phenomenological model [29] defines the threshold energy for the creation of thermalized electron-hole pairs in semiconductors crystals as $E_{eh} = 2.8E_g + E_{LO}$. Taking into account the value of $E_g = 3.8$ eV [31] and $E_{LO} = 0.044$ eV [33] the pair creation energy for ZnS is 10.7 eV. Electron-hole pairs created by photons of higher energy can generate secondary excitations through a process called photon multiplication. The number of such excitations increases with the photon energy, causing a gradual increase of the luminescence yield.

3.2. Scintillation properties

The temperature dependence of the scintillation response of ZnS-Ag/⁶LiF, measured using α -particle excitation, is shown in Fig. 3. It is found that the scintillation response under α -particle excitation shows little change over the temperature interval, as opposed to the luminescence emission intensity under excitation with monochromatic VUV photons (see Fig. 1). Such a difference associated with excitation conditions is often observed in luminescence materials [34,35]. It is generally interpreted as due to the difference in the distribution of excitation density over the volume

Table 1

Parameter of scintillation kinetics of ZnS-Ag/⁶LiF at different temperatures obtained from the fit to three exponential functions (A_i and τ_i are amplitudes and decay time constants).

T (K)	A_1	τ_1 (μ s)	A_2	τ_2 (μ s)	A_3	τ_3 (μ s)
295	0.84	4.52 ± 0.07	0.14	17.3 ± 1.6	0.02	82 ± 10
200	0.84	3.70 ± 0.04	0.14	16.8 ± 1.8	0.02	95 ± 20
100	0.84	3.80 ± 0.07	0.14	17.5 ± 1.3	0.02	119 ± 29
7	0.86	3.35 ± 0.05	0.13	17.8 ± 1.3	0.02	109 ± 23

of the material. Monochromatic VUV photons create electron-hole pairs in a thin surface layer (ca. 10 nm) with high concentration of non-radiative centers that facilitates quenching processes. On the other hand α -particles can penetrate a few micrometers into materials. Taking into account typical diffusion lengths of electron-hole pairs (< 100 nm [32]) the majority of created electron-hole pairs recombine within the bulk of the crystal where they are not affected by surface quenching processes.

Measurements of the kinetics of scintillation decay provide further insight into the scintillation mechanism of ZnS-Ag. Fig. 4 shows the scintillation decay curves of ZnS-Ag/⁶LiF at 295 and 7 K. It has been observed that the shape of the scintillation curves is largely unaffected by cooling and they exhibit recombination character over the full temperature range. For quantitative analysis, the recombination decay curve is often approximated by the sum of several exponential functions $f(t) = y_0 + \sum_i A_i \exp(-t/\tau_i)$, where y_0 is background, A_i and τ_i are amplitudes and decay time constants. The fit results are shown in Fig. 4 and fit parameters are listed in Table 1.

Inspection of the data compiled in Table 1 gives that cooling has only a very marginal effect on the scintillation decay kinetics of ZnS-Ag. It is only the first decay constant τ_1 which experiences a certain decrease, while all other parameters remain constant within the error. Altogether this is consistent with the observed temperature stability of scintillation light response and proposed interpretation since the changes in the decay kinetics and emission intensity are controlled by the same mechanisms.

4. Conclusion

We measured the excitation spectra of ZnS-Ag/⁶LiF over the 3.5–17 eV energy range and suggested their interpretation. The main features in the excitation spectra of ZnS-Ag are explained in terms of the manifestation of three principal effects: (i) the band structure of ZnS, (ii) the non-radiative surface recombination and (iii) the photon multiplication.

For the first time, the scintillation light response and kinetics of ZnS-Ag/⁶LiF have been measured over the temperature range 7–295 K. It has been shown that temperature has no significant effect on the scintillation characteristics. Light output and decay curve exhibit small changes with cooling. Thus, it is now confirmed that ZnS-Ag/⁶LiF is an adequate scintillation detector that can be used over a very wide temperature range. This finding prepares the ground for potential applications of this material as a neutron detector at cryogenic experiments.

Acknowledgments

The authors are grateful to Dr. Nigel Rhodes for providing the sample of ZnS-Ag/⁶LiF scintillator used in this study. The research leading to these results has received funding from The European Community's Seventh Framework Programme (FP7/2007-2013) under Grant agreement No. 312284.

References

- [1] W. Crookes, Proc. R. Soc. Lond. 71 (1903) 405.
- [2] M. Nikl, Meas. Sci. Technol. 17 (2006) R37.
- [3] C.W.E. Wan Eijk, Nucl. Instr. Meth. A. 477 (2002) 383.
- [4] E. Rutherford, Philos. Mag. 21 (1911) 669.
- [5] L. Ozawa, M. Itoh, Chem. Rev. 103 (2003) 3835.
- [6] T. Hoshina, H. Kawai, Jpn. J. Appl. Phys. 19 (1980) 267.
- [7] Y. Uehara, Chem. Phys. 62 (1975) 2982.
- [8] A.M. Gurvich, Introduction to Physical Chemistry of Crystal Phosphors, Moscow Higher School, 1982, (in Russian).
- [9] S. Shionoya, W.W. Yen, Phosphor Handbook, CRC Press, Boca Raton, 1999.
- [10] A. Lakshmanan, Luminescence and Display Phosphors: Phenomena and Applications, Nova Science Publishers, New York, 2008.
- [11] L. Romero, J. Campos, Phys. Stat. Sol. A 67 (1981) 259.
- [12] L.N. Tripatni, B.R. Chaubery, C.D. Mishra, U.N. Pandey, Phys. Lett. 86 (1981) 251.
- [13] E. Legler, W. Attwenger, F. May, G. Quittner, Rev. Sci. Instrum. 36 (1965) 1167.
- [14] Neutron Imaging and Applications, A Reference for the Imaging Community, in: I.S. Anderson, R. McGreevy, H. Bilheux (Eds.), Springer, 2009, p. 400.
- [15] N.J. Rhodes, E.M. Schooneveld, R.S. Eccleston, Nucl. Instr. Meth. A 529 (2004) 243.
- [16] T. Tojo, T. Nakajima, Nucl. Instr. Meth. A. 53 (1967) 163.
- [17] S.N. Kraitor, K.K. Koshaeva, Zhurnal Prikladnoi Spektroskopii 10 (1969) 638.
- [18] M. Matsubayashi, M. Katagiri, Nucl. Instr. Meth. A 529 (2004) 389.
- [19] M. Katagiri, T. Nakamura, M. Ebine, A. Birumachi, S. Sato, E.M. Schooneveld, N.J. Rhodes, Nucl. Instr. Meth. A 573 (2007) 149.
- [20] H. Kraus, E. Armengaud, M. Bauer M., et al., Dark Energy and Dark Matter: Observations, Experiments and Theories, 36, EAS Publication Series <http://dx.doi.org/10.1051/eas/0936035>, pp. 249–255.
- [21] C.A. Baker, S.N. Balashov, V. Francis, et al., J. Phys.: Conf. Ser. 251 (2010) 012055, <http://dx.doi.org/10.1088/1742-6596/251/1/012055>.
- [22] V.B. Mikhailik, H. Kraus, Phys. Stat. Sol. B 247 (2010) 1583.
- [23] H. Kraus, V.B. Mikhailik, Nucl. Instr. Meth. A 621 (2010) 395.
- [24] H. Kraus, V.B. Mikhailik, D. Wahl, Nucl. Instr. Meth. A 553 (2005) 522.
- [25] G. Zimmerer, Radiat. Meas. 42 (2007) 859.
- [26] J.K. Berkowitz, J.A. Olsen, J. Lumin. 50 (1991) 111.
- [27] W. Luo, S. Ismail-Beigi, M.L. Cohen, S.G. Louie, Phys. Rev. B 66 (2002) 195215.
- [28] L. Ley, R.A. Pollak, F.R. McFecly, S.I. Kowalczyk, D.A. Shirley, Phys. Rev. B 9 (1974) 600.
- [29] P.A. Rodnyi, P. Dorenbos, C.W.E. van Eijk, Phys. Stat. Sol. B 187 (1995) 15.
- [30] V.V. Mikhailin, A.N. Belsky, I.A. Kamenskikh, et al., Nucl. Instr. Meth. A 486 (2002) 367.
- [31] W. Lehmann, J. Electrochem. Soc. 118 (1971) 477.
- [32] E.L. Benitez, D.E. Husk, S.E. Schnatterly, C. Tarrío, J. Appl. Phys. 70 (1991) 3256.
- [33] Y.-M. Yu, M.-H. Hyun, S. Nam, et al., J. Appl. Phys. 91 (2002) 9429.
- [34] A.E.R. Malins, N.R.J. Poolton, F.M. Quinn, O. Johnsen, P.N. Denby, J. Phys. D: Appl. Phys. 37 (2004) 1439.
- [35] V.B. Mikhailik, H. Kraus, G. Miller, M.S. Mykhaylyk, D. Wahl, J. Appl. Phys. 97 (2005) 083523.